ISSN 1340-3745

ICRR

ICRR-Report-359-96-10

Kamiokande and Super-Kamiokande

Y. Totsuka

Invited Talks at the IV International Workshop on Theoretical and Phenomenological Aspects of Underground Physics-TAUP 95, Toledo, September, 1995, and the II Rencontres du Vietnam, Ho Chi Minh City, October, 1995.

(March, 1996)

INSTITUTE FOR COSMIC RAY RESEARCH
UNIVERSITY OF TOKYO
3-2-1 Midori-cho, Tanashi, Tokyo 188, Japan

KAMIOKANDE AND SUPER-KAMIOKANDE

Y. Totsuka
Institute for Cosmic Ray Research, University of Tokyo
3-2-1 Midoricho, Tanashi, 188 Tokyo, Japan

1. INTRODUCTION

A 3,000 ton water Čerenkov detector, Kamiokande, was built and became operational in 1983. Its primary objective was to search for proton decay, which at that time was one of the hottest topics in particle physics. After a year of unsuccessful search the lower limit of proton lifetime had already exceeded the theoretical prediction. We therefore decided to modify and improve the Kamiokande detector to observe solar neutrinos. A 10 MeV electron which could be produced by solar neutrinos yields only a 100th of Čerenkov light compared with a proton decay to $e^+\pi^0$. Hence in order to achieve the threshold energy below 10 MeV it was essential to have the high efficiency of light collection and to sufficiently reduce the background. Dominant background turned out to be radioactive elements dissolved in the water and gamma rays coming from the surrounding rock. Two measures were undertaken to eliminate these backgrounds: (i) installation of an improved water-purification system and isolation of the water from the ambient air (to avoid absorption of Rn gas), and (ii) construction of a 1,500 ton outer detector completely surrounding the 3,000 ton inner part with water thickness of $1.3 \sim 2.2$ m.

After two years of difficult work, Kamiokande became operational near the end of 1986. Initially the trigger threshold was set to 7.5 MeV and the analysis was made for events with visible energies larger than 9.3 MeV. Three months later we catched totally unexpected signals, antielectron neutrinos that had flown 16,000 years from the supernova, SN1987A, in the Large Magellanic Cloud. This observation dramatically confirmed the ability of the water Čerenkov technique even for detection of (anti-)neutrinos

as low as 7.5 MeV.

The experiment for solar neutrinos went smoothly after the excitement of SN1987A had subsided. Radioactive backgrounds were reduced to a manageable level. The analysis, however, encountered a new source of background, radioactive nuclei(^{12}B, ^{12}N, ^{16}N etc.), which were break-up products of oxygen nuclei hit by cosmic-ray muons. They had to be removed off-line by imposing various cuts in the data, but even after the tight cuts they remained as the most severe background above visible energies (E_{vis}) of 8 MeV.

Atmospheric neutrinos dominate over those of other sources for $E_{vis} \geq 100$ MeV, and they are the largest and perhaps the only background for a search of proton decay. It is quite natural that we, p-decay searchers, had to study atmospheric neutrinos in a close scrutiny. We developed a method to discriminate between electron and muon, i.e. particle-identification, to reduce atmospheric-neutrino events that otherwise faked proton decay. Applying this technique to single-Čerenkov ring events we found, to our great surprise already in 1988, that the observed μ/e ratio was significantly smaller for $E_{vis} < 1.3$ GeV than the simple expectation of $\mu/e \approx 2$. Single Čerenkov rings of μ and e are mostly produced by quasi-elastic scattering of ν_μ and ν_e, respectively. They are produced by decay of $\pi^\pm \rightarrow \mu^\pm \nu_\mu$ and subsequently by decay of $\mu^\pm \rightarrow e^\pm \nu_e \nu_\mu$ at low energies, resulting in $\nu_\mu/\nu_e = 2$. Hence $\mu/e \approx 2$. This argument is obviously free from inherent uncertainties in the flux of primary cosmic rays and nuclear interactions. Therefore the abnormal μ/e ratio strongly hints neutrino oscillations.

Super-Kamiokande is a 50,000 ton water Čerenkov detector with the light collection efficiency twice as good as that of Kamiokande. Moreover the photomultipliers with 50 cm diameter have charge and timing resolutions better by a factor of two than those of Kamiokande. Considering the light attenuation length in water of several tens of meters, Super-Kamiokande has an ultimate volume, namely even if a detector larger than Super-Kamiokande were built, one could not see the whole volume because the path length of light is longer than the attenuation length.

We built the Super-Kamiokande detector in order to further investigate the solar-neutrino problem and also the atmospheric-neutrino anomaly, though, I have to confess, the original design was optimized for a search of proton decay. Great volume and excellent resolution of Super-Kamiokande will contribute to clarify these important and interesting issues.

2. SOLAR NEUTRINOS

We brought to an end Kamiokande's observation of solar neutrinos in February, 1995, by which time we had already accumulated 2079 live-time days of data. The observational period covered almost an entire period of the solar cycle 22 which had a

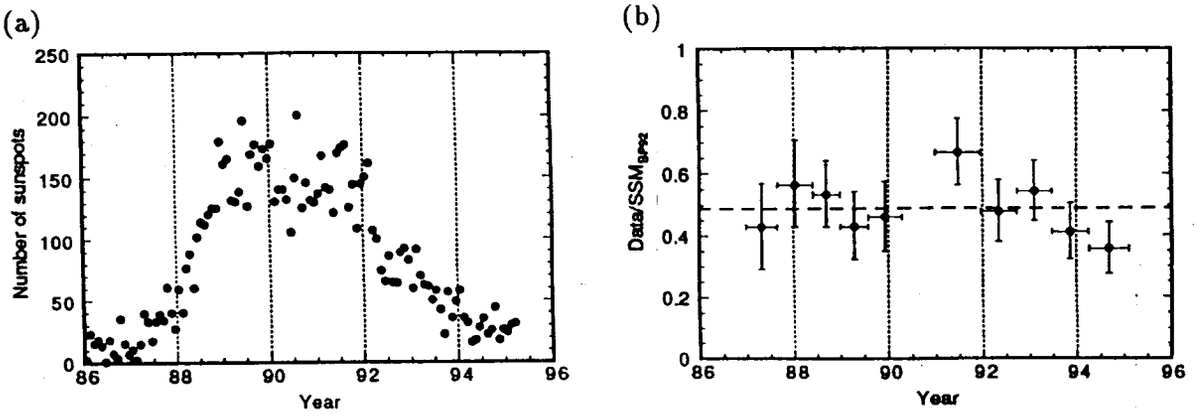

Figure 1: a: Variation of sunspot numbers in the solar cycle 22. b: The flux ratio of the sub-divided Kamiokande data to the SSM prediction. Each data point consists approximately of 200 days of data.

maximum activity around the year 1990 as shown in Fig.1a.

Kamiokande's high collection efficiency of Čerenkov light (25% coverage × 20% quantum efficiency ≈ 5% overall efficiency) enabled us to lower the observable energies (E_{vis}) down to 5 MeV, although the background problem did not allow us to analyze those with $E_{vis} < 7$ MeV. This analysis threshold was initially 9.3 MeV and, as the radioactive contamination decreased, was lowered progressively to 7 MeV.

We used the reaction $\nu_e + e \rightarrow \nu_e + e$ to detect solar neutrinos (ν_e). The electrons were scattered in the forward direction ($\theta \leq \sqrt{2m_e/E_\nu}$ when $E_\nu \gg m_e$), and they emitted Čerenkov light. These Čerenkov photons were received by the PMT's. For example a 10 MeV electron gave signals to 40 PMT's at the later phase of the experiment, Kamiokande-III(K-III). The number of hit PMT's, after corrections of transparency, etc., was a good measure of the electron energy or equivalently visible energy E_{vis}.

Since the observed electrons had a steeply falling spectrum in the energy range of 5 ~ 15 MeV, the key calibration for the Kamiokande detector was the absolute determination of E_{vis} or the proportionality coefficient (hits/MeV). To do this we used gamma rays of about 9 MeV produced by the reaction Ni(n_{th}, γ)Ni, n_{th} being neutrons from Cf fissions thermalized in water. The accuracy was found to be better than 3%. Gamma rays from the same source were also used to determine the directional resolution, which was correctly reproduced by a Monte Carlo simulation, which in turn gave the directional resolution of 26 ± 4 deg for a 10 MeV electron.

As mentioned above, we had to eliminate spallation products among the low-energy events. We made a variety of cuts depending on the total pulse hight, time and spatial correlation of muons preceding the low-energy events. It, however, was not possible to completely eliminate these backgrounds and to further improve the signal-to-noise ratio, we employed the distribution of the electron scattering angle θ_{sun}. The distribution for

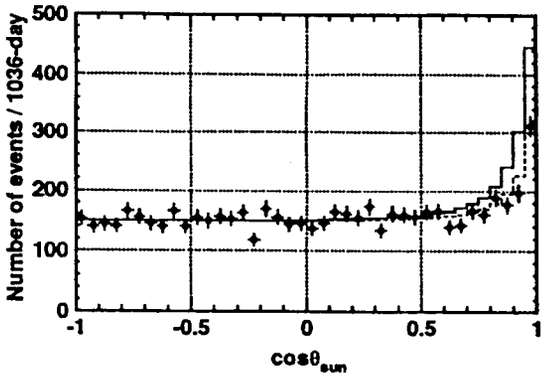

Figure 2: The $\cos\theta_{sun}$ distribution of the K-III final data (1036 days). The solid line is a flat background plus the expected yield from the SSM (BP_{92}). The dashed line is the best fit by adjusting the solar neutrino yield but leaving the histogram shape unchanged.

the K-III final data sample ($E_{vis} > 7$ MeV) is shown in Fig.2.

A prominent forward peak is clearly visible, which was obviously produced by solar neutrinos. The signal was extracted by fitting the whole spectrum with $a + bf(\theta_{sun})$, in which a corresponds to the flat background, $f(\theta_{sun})$ is the forward peak estimated by the standard solar model (SSM), the neutrino-electron scattering cross-section and the directional resolution, and finally b is the fraction of the observed number of solar-neutrino events compared with the SSM prediction. It is b that we wish to obtain. The electron energy distribution, namely $b(E_{vis})$, was also obtained by applying the same procedure to the data sub-samples with specified energy bins. Similarly we obtained b(day), b(night) and also a long-term variation of the b.

The results are presented in the following:[1]

(1) Solar neutrino flux

Adopting Bahcall-and-Pinsonneault's SSM (hereafter BP_{92}),[2] we obtained

$$b \equiv \frac{Data}{BP_{92}} = 0.496^{+0.044}_{-0.042} \pm 0.048,$$

based on the live-time of 2079 days (449, 594, 200 and 836 days for E_{vis} >9.3, 7.5, 7.5 and 7.0 MeV, respectively). This can be translated to the observed solar-neutrino flux of $2.82^{+0.25}_{-0.24} \pm 0.27 \times 10^6\,\mathrm{cm}^{-2}\mathrm{s}^{-1}$, assuming that the neutrino energy spectrum is the one predicted by the ^{8}B beta decay.

(2) Electron energy spectrum

Figure 3 shows the resultant $b(E_{vis})$ normalized to the BP_{92}. It is seen that the spectrum shape is consistent with theory, though the statistical uncertainties are too large to draw a meaningful conclusion.

(3) Day-night variation

Figure 4 shows the result, in which δ_{sun} is the anti-zenith angle ($\delta_{sun} = 0$ corresponds

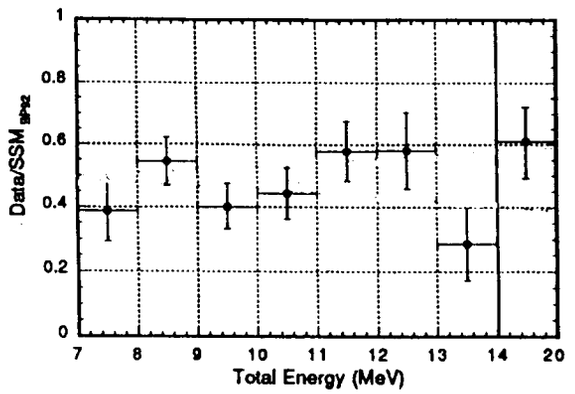

Figure 3: The recoil electron energy spectrum. The flux ratio of the Kamiokande data to the SSM (BP_{92}) prediction is shown.

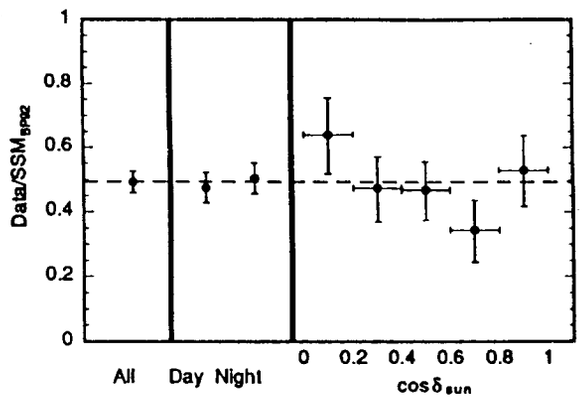

Figure 4: The flux ratio of the Kamiokande data to the SSM (BP_{92}) in the daytime and the nighttime. The data in the nighttime is further divided into five corresponding to the anti-zenith angle δ_{sun} (vertically upward for $\delta_{sun} = 0$).

to the vertically upward direction.) There is no day-night variation within statistical uncertainties.

(4) Long-term variation

Figure 1b shows the result for a period from December 1986 till February 1995, compared with the variation in the number of sunspots. One sees no correlation between data and number of sunspots, as it should be.

All of the results (1) $\sim$ (4) are subject to the scrutiny of various theoretical considerations that may solve the solar-neutrino problem. Especially the result on the above (1) and (3) have extensively been used for the MSW mechanism. The result on the electron energy spectrum (2) was largely ignored, partly because the statistical uncertainties were too large and also it was not easy to implement the detector effects in theoretical predictions. We, however, believe that the precise measurement of the electron energy spectrum will be a key to disentangle the solar-neutrino problem, and indeed the construction of the Super-Kamiokande detector was motivated by this.

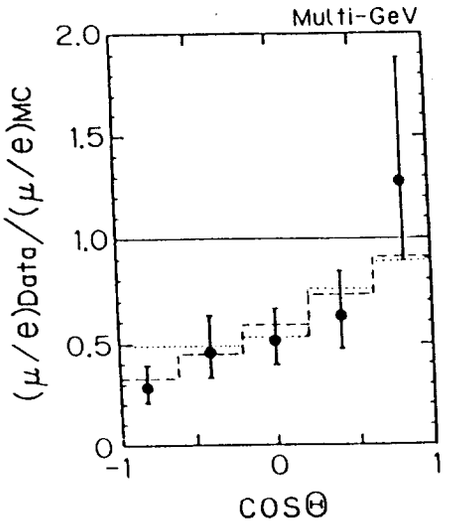

Figure 5: The zenith angle distribution of $(\mu/e)_{data}/(\mu/e)_{MC}$ for the multi-GeV data.

3. SOME COMMENTS ON ATMOSPHERIC NEUTRINOS

The momentum range that we were interested in was above 100 MeV/c and 200 MeV/c for e and μ, respectively. The observed events were further divided to either those that had single Čerenkov rings, $E_{vis} < 1330$ MeV (note for muons $E_{vis} = p_\mu - 200$ MeV) and all secondary particles fully contained in the detector (we call this data sample sub-GeV) or those that had single or prominent single (more than 80% of the total E_{vis}) Čerenkov rings, $E_{vis} > 1330$ MeV and secondary particles either fully contained or partially contained (we call this data set multi-GeV).

We have already published the results corresponding to the detector exposure of 8.2 kton·yr.[3] The final results based on the data till February, 1995 will soon be published. In order to cancel the large uncertainty in the absolute atmospheric ν_e, ν_μ fluxes, we always consider the ratio of μ to e, $(\mu/e)_{data}$ and $(\mu/e)_{MC}$ for the observed and the Monte-Carlo simulated data, respectively. Then the results from Kamiokande may be summarized as follows:

(1) sub-GeV energy range

$$(\mu/e)_{data}/(\mu/e)_{MC} = 0.60^{+0.06}_{-0.05} \pm 0.05.$$

(2) multi-GeV energy range

$$(\mu/e)_{data}/(\mu/e)_{MC} = 0.57^{+0.08}_{-0.07} \pm 0.07.$$

The zenith angle distribution is strongly distorted as shown in Fig.5. Specifically, $(\mu/e)_{data}/(\mu/e)_{MC} = 1.3^{+0.6}_{-0.4}$ and 0.3 ± 0.1 for $\cos\Theta = 0.6 \sim 1$ and $-1 \sim -0.6$, respectively ($\Theta = 0$ corresponds to the downward direction). Though the statistical

uncertainties are large, a strong suppression of ν_μ occurs for upward-going neutrinos which traversed the earth material of about 10,000 km.

These results, if confirmed, cannot simply be accounted for by modifying nuclear interactions and/or the primary cosmic-ray spectrum, and a plausible explanation could be due to neutrino oscillations of either $\nu_\mu \leftrightarrow \nu_e$ or $\nu_\mu \leftrightarrow \nu_\tau$ with an oscillation length of the order of $100 \sim 1000$ km and a large mixing angle.

This implication is so important that we looked for every systematics related to the Kamiokande detector and especially we decided to experimentally confirm Kamiokande's capability of e and μ identification.

It was recently claimed[4] that neutrons, which were produced in the surrounding rock by cosmic-ray μ's, scattered in large angles (μ's should not be seen), punched through the water shield of Kamiokande without any signals there, produced π^0's in the inner detector and finally these π^0's were misidentified as electrons. Although this scenario was extremely unlikely, we decided to study this hypothetical process. We comment on these two studies.

(1) Particle identification (ID) capability

We carried out a test-beam experiment to measure the mis-ID probabilities for e and μ and to compare them with the Monte Carlo estimates. A 1000 ton water Čerenkov detector was built at KEK, in which PMT's and their array were exactly the same as those of Kamiokande. e, μ^- and π^- beams of momenta $100 \sim 1000$ MeV/c were injected at 10 different positions in the 1000 ton detector. We analyzed almost 200 sets of data (position × momentum bins) in just the same way as for Kamiokande's atmospheric-neutrino data. The results based on the first three beam positions will soon be published.[5]

The essential point of the particle-ID is to quantify the difference in the amount of diffuse light outside the Čerenkov angle. We calculate the following logarithmic functions for e-likeness and μ-likeness:

$$L_e = \log_{10}[\,\Pi_{\theta_i<1.5\theta_c} \quad P(N_i, N_i^e)],$$

$$L_\mu = \log_{10}[\,\Pi_{\theta_i<1.5\theta_c} \quad P(N_i, N_i^\mu)],$$

where $P(N_i, N_i^e)$ is the probability that the i-th PMT has the number of photoelectrons N_i while it is expected to have the average number N_i^e if the particle is an electron. All the PMTs are considered if they are located within 1.5 times the Čerenkov angle θ_c.[5]

We show in Fig.6 the distribution of $L_\mu - L_e$ measured for beams of 300 MeV/c e (open histogram) and 500 MeV/c μ (hatched histogram). Note that the two beams have approximately the same total photoelectrons. e and μ are indeed well separated. Now by assigning a particle as e if $L_\mu - L_e < 0$ and as μ if $L_\mu - L_e > 0$, we finally obtain the mis-ID probabilities, which are shown in Fig.7 for three incident positions

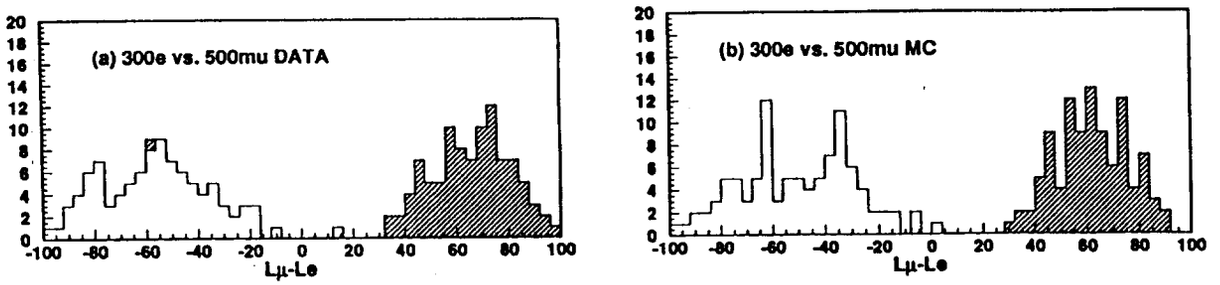

Figure 6: The $[L_\mu - L_e]$ distribution of (a) data and (b) Monte-Carlo samples for e(300 MeV/c) and μ(500 MeV/c) at the position S. The e and μ data samples have about the same total photoelectrons.

S(injection point 7.8 m away from the PMT wall), C(4.8 m from the PMT wall) and D(2.1,m from the PMT wall, corresponding to the near edge of Kamiokande's fiducial volume). The mis-ID probabilities are indeed very small and more importantly they are well reproduced by the Monte Carlo simulation. Hence this experiment has confirmed the validity of the Monte Carlo simulation currently being used for Kamiokande, and thus the validity of the particle-ID.

(2) π^0 contamination in the electron data

We first searched for π^0's in the sub-GeV data sample (7.0 kt·yr). We selected two-Čerenkov-ring events and applied the particle-ID program to pick up only e-like rings. The invariant-mass distribution of the pairs is shown in Fig.8 together with the Monte Carlo estimate. A peak on the π^0 mass is clearly seen. The yield is somewhat less than what is expected, but this should not be taken seriously because of large uncertainties in cross-sections of the neutral-current π^0 production. Events in the region of $90 \sim 180$ MeV were selected as π^0-like, the number of which was 37, while during the same period we observed 225 e-like events ($p_e > 100$ MeV/c) and 212 μ-like events ($p_\mu > 200$ MeV/c).

Next we estimate two kinds of efficiency, π^0's identified as π^0-like and π^0's misidentified as e-like (i.e., single-ring and particle-ID as e-like). A large number of atmospheric-neutrino events were generated with Kamiokande's Monte Carlo simulator and the identical selection criteria for π^0 and e were applied to these artificial data. The two kinds of efficiency were shown in Fig.9 as a function of π^0 momenta. Weighting them with the momentum distribution of atmospheric π^0's, the resultant efficiency was, $\varepsilon_{\pi^0/\pi^0} = 0.77$ and $\varepsilon_{\pi^0/e} = 0.17$. Therefore from the observed 37 π^0's, we conclude that the π^0 contamination in the e-like sample is $37 \times 0.17/0.77 = 8.0 \pm 1.3$ events, which are only 4% of the total e-like events.

Of course we expect that most of these events are of atmospheric-neutrino origin and the contribution from external neutrons should be much smaller. A more careful analysis was made which took into account the attenuation of π^0's as their production points went deep in the detector. Namely we analyzed excess events near the PMT wall

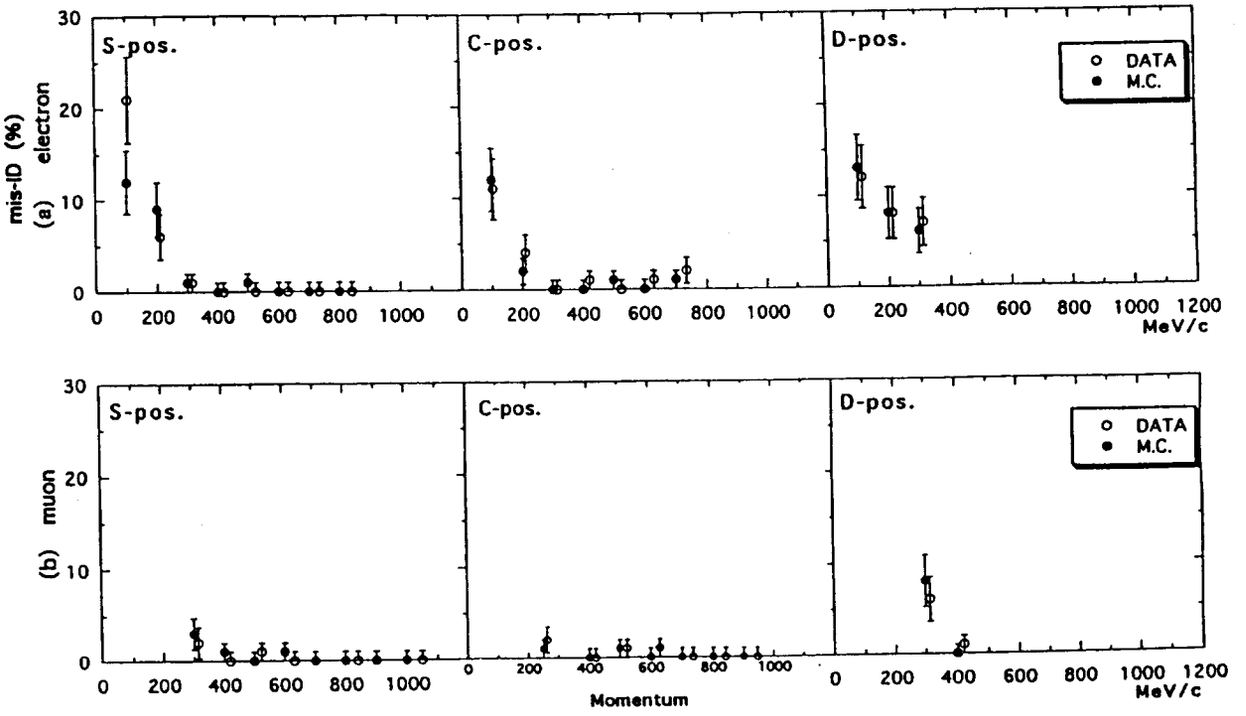

Figure 7: The mis-ID probabilities for (a) e and (b) μ at the three points of beam incidence, compared with the Monte-Carlo estimates.

which might exist above the flat atmospheric-neutrino background. The number of π^0's of neutron origin was then found to be 4.3 ± 10.2 and hence the faked e-like events were only 0.8 ± 2.0, which correspond to only 0.4% of the total e-like events. The conclusion is, as we expected, the contamination of π^0's of external-neutron origin was negligible.

As a further check, we generated neutrons with their flux claimed in ref.4, simulated their traverse through the water shield and their π^0 production in the Kamiokande detetor. We analysed these artificial data and compared the selected events with the observed ones. Figure 10 shows the event rates as a function of the distance between π^0's and the colsest PMT wall. It is seen that the claimed n-flux is grossly overstimated and hence the argument in ref.4 is incorrect.[6]

We believe, after having studied the above two issues, that the atmospheric-neutrino anomaly becomes even more serious.

4. CURRENT STATUS OF SUPER-KAMIOKANDE

The Super-Kamiokande detector is a 50,000 ton water Čerenkov detector, and its construction is at the final stage as of February 1996. The tank has a dimension of 39.3 mϕ × 42 mh. Water is to be filled to the height of 41.4 m. 11,146 PMT's with 20″ϕ are placed with their photocathode inward on the inner cylindrical wall of 33.8 mϕ × 36mh with the surface density of 2PMT/m^2. The space between the PMT wall and the

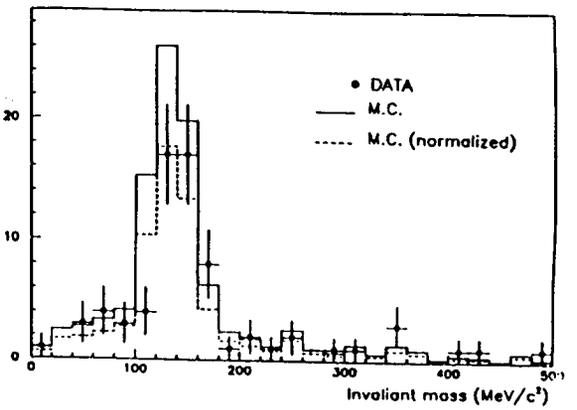

Figure 8: The invariant-mass distribution of two-Čerenkov ring events with both rings identified as e-like in Kamiokande's atmospheric-neutrino data. A mass range of 90–180 MeV is assumed for π^0-like events.

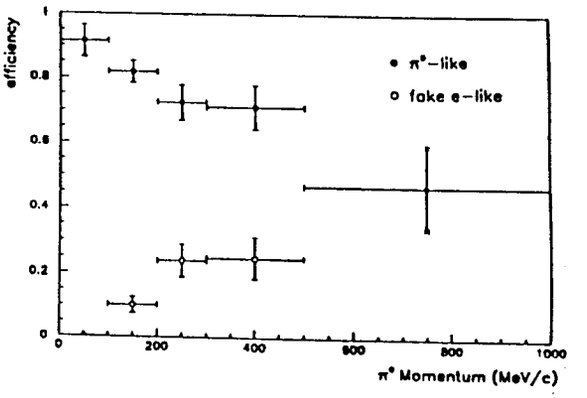

Figure 9: Efficiency of π^0-identification (full circle) and of mis-identification as e-like (open circle) for single π^0's produced by atmospheric-neutrinos. This is the result from a Monte-Carlo study.

tank wall is filled with water and equipped with about 1800 PMT's with $8''\phi$ to tag incoming muons and particles that punched through the inner detector.

All the PMT's except the last 400 had already been mounted by December 1995, and water filling started on 20 December 1995. Test data-taking has started since January 1996 in parallel with water filling. We have sofar encountered no serious problems. The full operation will begin on 1 April 1996 as originally scheduled. Figure 11 is a photo of the PMT array being slowly swallowed by pure water.

We believe that in coming years Super-Kamiokande will contribute much to solve the solar- and atmospheric-neutrino problems, and of course we have a high hope that proton decay and the next supernova will soon be discovered.

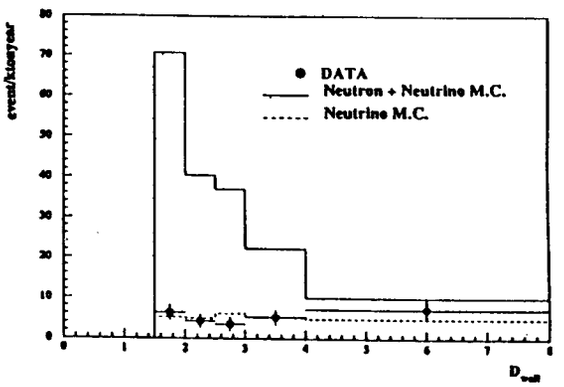

Figure 10: Comparison between the observed π^0 rate and the one expected from ref.4 (solid line). D_{wall} is a distance between π^0's and the closest PMT wall.

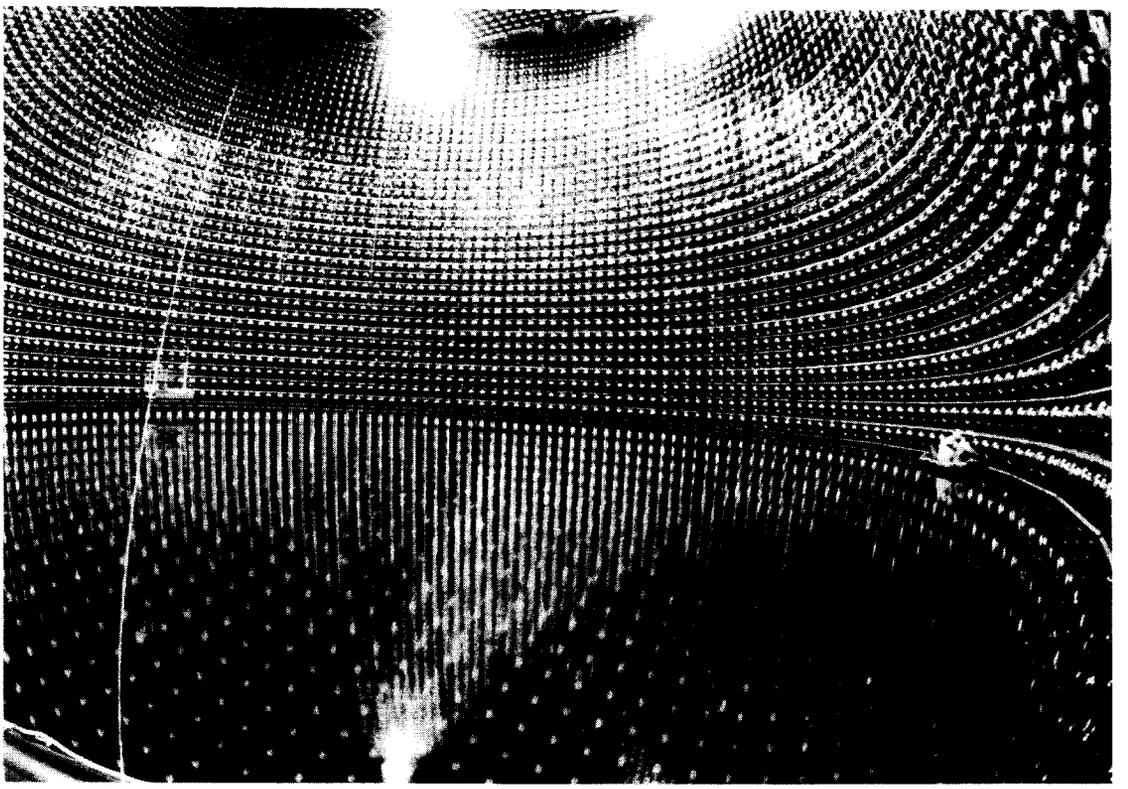

Figure 11: A photo of the PMT array inside the Super-Kamiokande detector. The water surface is also seen.

REFERENCES

1. to be published in 1996.
2. J.N. Bahcall and M.H. Pinsonneault, Rev. Mod. Phys. **64**, 885 (1992).
3. Y. Fukuda etal., Phys. Lett. **B335**, 237(1994).
4. O.G. Ryazhskaya, Gran Sasso preprint LNGS-94/110.
5. S. Kasuga etal., to appear in Phys. Lett. B(1996).
6. K. Okumura etal., to be published in 1996.